NASA TECHNICAL NOTE

NASA TN D-3918

NASA TN D-3918

COMPRESSIVE BEHAVIOR OF PLATES FABRICATED FROM GLASS FILAMENTS AND EPOXY RESIN

by John G. Davis, Jr., and George W. Zender

Langley Research Center
Langley Station, Hampton, Va.

NATIONAL AERONAUTICS AND SPACE ADMINISTRATION • WASHINGTON, D. C. • APRIL 1967

NASA TN D-3918

COMPRESSIVE BEHAVIOR OF PLATES FABRICATED FROM GLASS FILAMENTS AND EPOXY RESIN

By John G. Davis, Jr., and George W. Zender

Langley Research Center
Langley Station, Hampton, Va.

NATIONAL AERONAUTICS AND SPACE ADMINISTRATION

For sale by the Clearinghouse for Federal Scientific and Technical Information
Springfield, Virginia 22151 – CFSTI price $3.00

COMPRESSIVE BEHAVIOR OF PLATES FABRICATED FROM GLASS FILAMENTS AND EPOXY RESIN

By John G. Davis, Jr., and George W. Zender
Langley Research Center

SUMMARY

Young's modulus, buckling stress, and maximum strength were determined experimentally for 15 glass-filament-reinforced plastic plates of laminated isotropic construction containing either 12 or 18 laminae. Experimentally determined values of Young's modulus and buckling stress are in reasonable agreement with theoretical calculations. The stress—unit-shortening curve for the plates in the post-buckling region can adequately be predicted by conventional theory for metallic plates. However, delamination occurs at loads below the theoretical compressive strength predicted by an effective width formula that is often used to predict the maximum strength of metal plates. In using an effective width formula to predict maximum strength, it was assumed that failure occurs when the edge stress of the buckled plate equals the delamination stress of the unbuckled compression test specimen. On the basis of strength and modulus data obtained in this study, it is shown that the glass-epoxy composite is competitive as a lightweight material with aluminum in applications where plate buckling strength or crushing strength is the design criterion.

INTRODUCTION

The success of filament-wound motor cases has aroused interest in the application of filament-reinforced composites to the primary structures of aerospace vehicles. One area of interest concerns the ability of filament-reinforced composites to support compressive loads. Results, such as those reported in references 1 and 2, have indicated an inherent weakness of glass-epoxy laminates in compressive crushing tests and a need for data on the behavior of structural elements when subjected to compressive loads. Where compressive instability of shells is involved, studies such as those presented in references 3 and 4 have shown the importance of filament orientation in attaining efficient design. Since the structure of aerospace vehicles often involves compressively loaded flat-plate elements, a program was initiated to provide information on the behavior of glass-filament-reinforced plastic plates when subjected to in-plane compressive loads. The results of the investigation are included herein.

SYMBOLS

The units used for physical quantities defined in this paper are given in both the U.S. Customary Units and in the International System of Units (SI). Conversion factors pertinent to the present investigation are presented in the appendix and in reference 5.

a	length of plate between end supports, inch (meter)
b	width of plate between edge supports, inch (meter)
E	Young's modulus, pounds force/inch^2 (newtons/meter^2)
E_S	secant modulus, pounds force/inch^2 (newtons/meter^2)
N_X	compressive load per unit width, pounds force/inch (newtons/meter)
k_X	compressive buckling stress coefficient
t	plate thickness, inch (meter)
V	volume fraction, ratio of constituent volume to total volume
ϵ	strain
μ	Poisson's ratio
η	empirical factor (see eq. (4))
ρ	density, pounds mass/foot^3 (kilograms/meter^3)
σ	stress, pounds force/inch^2 (newtons/meter^2)
δ	buckle amplitude, inch (meter)

Subscripts:

cal	calculated value
cr	buckling

edge	refers to vertical edge of plate
exp	experimental
max	maximum
f	fiber
m	matrix
v	void
y	yield

TEST SPECIMENS

Fifteen laminated flat plates were fabricated from either 12 or 18 laminae of nonwoven E-glass filaments preimpregnated with epoxy resin. The plates were press-cured at 300° F (420° K) for a period of 1/2 hour and post-cured in an oven at 350° F (450° K) for 4 hours. The material properties of the glass and epoxy are listed in table I. The average volume fraction of filament V_f contained in each lamina is 47 percent, about 20 to 25 percent below the value of V_f in most rocket motor cases or pressure vessels. The effect of V_f on the efficiency of the glass-epoxy composite in plate buckling applications will be discussed subsequently.

Details of the plates are given in figure 1 in conjunction with table II. Successive laminae are oriented at a 60° angle so that the plate consists of filaments oriented at angles of 0°, 60°, and 120° with respect to the direction of loading and the midplane of the plate is a plane of symmetry. (See figs. 1 and 2.) Such construction is considered to be theoretically isotropic in the sense of gross behavior. (See, for example, ref. 6.) The sides of the plates near the ends were clamped with aluminum supports, as shown in figure 1, to prevent delamination of the ends during tests. The ends were finished flat, square, and parallel in an effort to achieve uniform loading over the ends by the testing machine. The value of thickness given in table II for each plate represents the average of 10 or more measurements. The maximum deviation in individual thickness measurements is within ±2 percent of the

TABLE I.- CONSTITUENT PROPERTIES

Material	E		μ	ρ	
	ksi	GN/m^2		lbm/in^3	Mg/m^3
Glass[a]	10 500	72.4	0.23	0.092	2.54
Epoxy[b]	590	4.1	.33	.0437	1.21

[a]Typical properties for E-glass filaments.
[b]Property values supplied by manufacturer.

TABLE II.- PLATE DIMENSIONS AND CONSTITUENT VOLUME FRACTIONS

Plate	t		b		V_f, percent	V_m, percent	V_v, percent	ρ	
	in.	cm	in.	cm				lbm/in^3	Mg/m^3
12 laminae									
1	0.119	0.302	3.60	9.15	45	51	4	0.0637	1.76
2	.120	.305	3.60	9.15	45	52	3	.0641	1.77
3	.120	.305	3.30	8.38	46	53	1	.0655	1.81
4	.121	.308	3.30	8.38	46	53	1	.0655	1.81
5	.120	.305	3.00	7.62	46	52	2	.0650	1.80
6	.121	.308	2.40	6.10	45	53	2	.0646	1.79
7	.120	.305	2.40	6.10	45	52	3	.0641	1.77
18 laminae									
8	0.179	0.455	4.00	10.16	46	53	1	0.0655	1.81
9	.177	.450	4.00	10.16	47	52	1	.0659	1.82
10	.179	.455	3.70	9.40	44	54	2	.0641	1.77
11	.176	.447	3.70	9.40	47	52	1	.0659	1.82
12	.162	.411	3.18	8.07	49	49	2	.0665	1.84
13	.167	.424	3.18	8.07	48	49	3	.0656	1.81
14	.161	.409	2.93	7.45	49	49	2	.0665	1.84
15	.156	.396	2.93	7.45	50	48	2	.0670	1.85

value listed in table II. The ratio of width to thickness for the plates b/t ranges from about 18 to 30. The values of volume fraction listed in table II were determined in the following manner from coupons cut from each plate. The weight and volume of each coupon were measured. Next the coupon was subjected to a temperature of 1100° F (865° K) for a period of 3 hours to decompose the epoxy resin. The residue (glass filaments) was weighed and the volume of glass filaments in the coupon calculated. The difference between the weight of the coupon and residue is the weight of the epoxy contained in the coupon and was used to compute the volume of epoxy in the coupon. Void volume was determined by subtracting the sum of the glass filament and epoxy volumes from the coupon volume. The experimental error in determining the volume of the coupon is such that the void volume fractions listed are probably only accurate to ±1.0 percent at best.

In order to determine a stress-strain curve and the compressive strength of the material from which the plates were fabricated, two "dog bone" type specimens described in ASTM method D695-63T (ref. 7, pp. 243-249) were fabricated. A photograph of the specimen and test support fixture is shown in figure 3.

TEST METHOD

The plates were subjected to compressive loads as shown in figure 4. The edges of the plate were supported by knife-edge type fixtures as shown in figures 4 and 5.

These fixtures were adjustable to accommodate plates of different thicknesses and were made of 17-4PH stainless steel heat treated to the H900 condition. In order to alleviate cutting into the relatively soft epoxy, a 0.0156-inch (0.04-cm) radius was provided on the contact edges of the fixture. (See fig. 5.) The fixtures were made 0.375 inch (0.95 cm) shorter than each plate in order that the testing machine load be supported by the plate except for friction loads which were assumed to be negligible.

A compressive load was applied continuously at a deformation rate of 0.05 in/min (21 μm/s) until the plate failed. (See figs. 6 and 7.) Shortening was measured by a linear direct-current differential transformer as shown in figure 4. Similar instruments measured the lateral displacement at five locations along a vertical line midway between the edge supports in order to detect the mode and extent of plate buckling. (See fig. 8.) Load and displacements were recorded at a virtually continuous rate in the Langley central digital data recording facility and selected measurements were monitored on an oscilloscope.

The dog bone type of compression specimens were loaded continuously at a strain rate of 0.005 per minute until the specimen failed. The strain was measured by foil-type strain gages bonded to each edge of the specimen with a room-temperature cure adhesive (fig. 3).

TEST RESULTS

The results of the plate tests are listed in table III. Typical curves of average stress on the plate plotted against unit-shortening and buckle amplitude are shown in figures 9, 10, and 11. The unit-shortening or edge strain was determined by dividing the total shortening of the plate by 10 inches. Values of unit shortening computed in this manner were in agreement with strains measured with wire-type strain gages used in a preliminary test. The buckle amplitude was determined in the manner shown in figure 12. The buckling stress (see figs. 9, 10, and 11) was determined from the stress—unit-shortening plot at the stress where a sharp reduction in slope appears. This change in slope is a result of the reduced stiffness of the plate due to buckling. As indicated on the stress—buckle-amplitude plots, the buckling stress determined by the "top of the knee" method is in agreement with the buckling stress indicated on the stress—unit-shortening curve. (See ref. 8.)

The initial slope of the stress—unit-shortening plot for each plate was determined and is listed under the column headed E_{exp} in table III. Since the stress-strain plots deviated slightly from linearity at stresses below the buckling stress, the secant modulus was determined at the buckling stress and is listed in table III under the column entitled E_s.

Failure of the plates consisted of a delamination accompanied by a loud noise and a sharp reduction in the load supported by the plate. The delamination appeared to be essentially between adjacent laminae of the plate in the area of the central portion of the plate. (See fig. 7.) The particular location of the onset of failure could not be identified because of the sudden occurrence of the delamination. The average stress at maximum load is listed in table III under the column entitled σ_{max}.

TABLE III.- EXPERIMENTAL AND COMPUTED RESULTS

Plate	E_{exp}		E_{cal}		$\frac{E_{exp} - E_{cal}}{E_{exp}}(100)$	$(\sigma_{cr})_{exp}$		$(\sigma_{cr})_{cal}$		k_x	a/b	b/t	E_s		σ_{max}	
	ksi	GN/m^2	ksi	GN/m^2		ksi	MN/m^2	ksi	MN/m^2				ksi	GN/m^2	ksi	MN/m^2
1	2 720	18.8	2 540	17.5	6.6	12.0	83	12.1	83	4.63	2.225	30.25	2 670	18.4	17.5	121
2	2 750	19.0	2 550	17.6	7.3	12.0	83	12.3	85	4.63	2.225	30.00	2 670	18.4	17.3	119
3	2 760	19.0	2 640	18.2	4.4	14.2	98	13.9	96	4.56	2.425	27.50	2 580	17.8	19.3	133
4	2 760	19.0	2 640	18.2	4.4	14.4	100	14.3	99	4.56	2.425	27.25	2 590	17.9	18.4	127
5	2 915	20.1	2 620	18.1	10.1	16.5	114	17.7	122	4.57	2.670	25.00	2 700	18.6	19.8	137
6	2 690	18.6	2 570	17.7	4.5	24.2	167	24.0	166	4.33	3.335	19.84	2 440	16.8	27.7	191
7	2 675	18.5	2 550	17.6	4.7	23.8	164	23.6	163	4.33	3.335	20.00	2 430	16.8	26.9	186
8	2 860	19.7	2 640	18.2	7.7	20.5	142	21.5	148	4.85	2.000	22.35	2 470	17.0	24.0	166
9	2 760	19.0	2 690	18.6	2.5	21.5	148	21.5	148	4.85	2.000	22.60	2 530	17.5	25.1	173
10	2 760	19.0	2 520	17.4	8.7	24.4	168	24.5	169	4.66	2.165	20.65	2 500	17.2	29.7	205
11	2 840	19.6	2 690	18.6	5.3	23.6	163	23.8	164	4.66	2.165	21.05	2 520	17.4	29.1	201
12	3 015	20.8	2 780	19.2	7.8	26.6	183	28.7	198	4.55	2.515	19.63	2 720	18.8	32.1	222
13	2 915	20.1	2 710	18.7	7.0	28.2	195	28.6	197	4.55	2.515	19.02	2 540	17.5	32.3	223
14	3 160	21.8	2 780	19.2	12.0	31.7	219	32.8	226	4.57	2.730	18.32	2 690	18.6	36.3	250
15	3 105	21.4	2 840	19.6	8.5	30.4	210	31.7	219	4.57	2.730	18.79	2 720	18.8	35.1	242

The results of the compression test of dog bone type of specimens are shown in figure 13 as the "stress-strain curve for material." The stress-strain curves for both specimens are identical within the accuracy of the plot shown in figure 13 and deviated somewhat from linearity. The average stress at maximum load for both specimens is approximately 45 ksi (310 MN/m^2). On the basis of uniform strain, the strain at failure of 0.019 corresponds to a stress of 200 ksi (1380 MN/m^2) in the glass filaments oriented in the direction of the load. Specimen failure was a consequence of delamination of the outer layer which extended from the ends of the specimen toward the center. (See fig. 3.) The average volume fraction of glass filament, epoxy, and void in the dog bone type of specimens was 45, 54, and 1 percent, respectively.

THEORETICAL ANALYSIS

Young's Modulus

Computation of the theoretical value of Young's modulus for each plate involved three steps. The first step consisted of accounting for the effect of voids in the epoxy on Young's modulus of the composite. This step was accomplished by employing an approximate method presented in reference 9. Young's modulus of the matrix was multiplied by

$$\frac{V_m}{V_m + V_v}$$

and the resulting value was used in the subsequent computations. The second step consisted of computing the elastic constants transverse and parallel to the filaments of a lamina. This computation was performed by using an analysis presented in reference 10. The analysis of reference 10 is based on the assumption that the filaments are randomly spaced in the matrix and yields upper and lower bounds on the five elastic constants. The bounds are coincident except for Young's modulus transverse to the filaments. The upper bound was used in subsequent computations. The third step consisted of using the elastic constants determined in step two to obtain the Young's modulus of the multilayered composite. In the analysis, the composite is assumed to be composed of anisotropic laminae that are bonded together at their respective interfaces. Coupling between extensional and bending stiffnesses was neglected. From a consideration of equilibrium and compatibility conditions of the bonded laminae, Young's modulus for the isotropic composite is obtained. (See, for example, ref. 11.) Computations in steps two and three were performed by a digital computer.

Plate Buckling

The theoretical buckling stress for each plate was computed from the equation

$$\sigma = \frac{k_x \pi^2 E_s}{12(1 - \mu^2)(b/t)^2} \tag{1}$$

The value of k_x for each plate was obtained from figure 3 of reference 12. In using reference 12 to determine k_x, a value of 8.00 inches (20.32 cm) was used for the plate length. This length was considered appropriate because observation of the test data indicated that the portion of the plate covered by the aluminum end supports remained essentially vertical during the test (fig. 1). Since the stress-strain curve for the isotropic glass-epoxy composite is nonlinear, the secant modulus E_s rather than the Young's

modulus appears in equation (1). This approximate method of accounting for plasticity, which is applicable for buckling stresses when the tangent and secant moduli do not differ substantially, is given in reference 13.

An alternate form of equation (1) that is often useful in comparing experimentally determined and computed buckling results is

$$\epsilon_{cr} = \frac{k_x \pi^2}{12\left(1 - \mu^2\right)(b/t)^2} \tag{2}$$

Post-Buckling Behavior of Isotropic Plates

The theoretical stress—unit-shortening curve for a buckled isotropic plate was computed with the aid of the following effective width formula:

$$\frac{\sigma}{\sigma_{edge}} = \eta\sqrt{\frac{\epsilon_{cr}}{\epsilon}} \tag{3}$$

which is presented in reference 14. The empirical factor η was evaluated from

$$\eta = 1 + 0.28\left(1 - \sqrt{\frac{\epsilon_{cr}}{\epsilon}}\right)^3 \tag{4}$$

The edge stress was obtained from the stress-strain curve of the material from which the plate was fabricated, that is, the test data for the dog bone type of specimen.

The following form of equation (3) was used to compute the theoretical maximum strength of the plates:

$$\sigma_{max} = \sqrt{\epsilon_{cr}}\left(\frac{\eta\sigma_{edge}}{\sqrt{\epsilon}}\right)_{max} \tag{5}$$

Inspection of the stress-strain curve for the material from which the plate was fabricated indicates that the quantity $\frac{\eta\sigma_{edge}}{\sqrt{\epsilon}}$ is maximum when the edge stress of the buckled plate equals the delamination stress of the dog bone type of specimen.

COMPARISON OF TEST RESULTS AND THEORY

Young's Modulus

A tabulation of the measured and computed values of Young's modulus for the 15 plates tested is given in table III. The largest matrix reduction factor

$$\frac{V_m}{V_m + V_v}$$

was 7.3 percent (plate 1). The corresponding value of Young's modulus of the composite is 2 percent less than the value computed without accounting for the effect of voids in the epoxy. Calculation of the percent difference

$$\frac{E_{exp} - E_{cal}}{E_{exp}} \times 100$$

between the experimentally determined and computed values indicates that the average difference is about 7 percent. As a result, it appears that the value of Young's modulus for filament-reinforced composites of laminated isotropic construction can adequately be predicted by existing theory.

Buckling Stress

A comparison of the experimentally determined and computed buckling stress for each plate tested is shown in figure 14 and table III. The values of k_x, a/b, b/t, and E_s utilized to compute the buckling stress of each plate are given in table III. A value of 0.29, determined from a preliminary test on the material from which the plates were fabricated, was used for Poisson's ratio in all plate-buckling calculations. A plot of the buckling strain ϵ_{cr} as a function of $(b/t)^2$ for two values of the plate-buckling coefficient k_x is shown in figure 14. Observations of table III and figure 14 clearly indicate that existing plate theory can be used to predict adequately the buckling stress of isotropic glass-filament-reinforced epoxy plates.

Post-Buckling Behavior

A comparison of the calculated and experimentally determined stress—unit-shortening curve in the post-buckling region is shown in figure 13. The theory and experiment are in good agreement until the plate delaminates. This delamination occurs at loads below the theoretical compressive strength predicted by the effective width formula used herein. In using equation (5), it was assumed that failure occurs when the edge

stress of the buckled plate equals the delamination stress of the unbuckled compression test specimen.

Although the dog bone type of specimens and the plates failed by delamination, each failed at a different stress level. The dog bone type of specimens failed by delaminations that extended from the specimen ends toward the center of the specimen. In the plates, delamination occurred in the area of the central portion of the plate. Delamination of the dog bone type of specimens may have been caused by end restraint at the specimen-platen interfaces (ref. 1). Delamination of the plates was likely due to shear failure precipitated by the shear stresses developed in the buckled plate.

MATERIALS COMPARISON

A comparison of the E-glass filament and epoxy resin composite material used in the study reported herein with aluminum, magnesium, titanium, and beryllium for aerospace structural applications follows. Material properties used in the comparison are listed in table IV. The strength and modulus properties shown for the isotropic glass-epoxy composite are based on tests reported herein. Since the volume fraction of glass V_f contained in the glass-epoxy composite used in this study was only 47 percent, about 20 to 25 less than the value of V_f in rocket motor cases or pressure vessels, the effect of V_f on the material efficiency parameter $\frac{\rho}{E^{1/3}}$ when plate buckling is the basis for comparison is shown in figure 15. Note that varying the volume fraction of glass from 20 to 75 percent has little effect on the efficiency of the isotropic glass-epoxy composite when plate buckling is the basis for comparison. Since 75 percent is about the upper practical limit of V_f for circular fibers, the present plates are representative of efficient design from the standpoint of compressive buckling for the glass-epoxy composite of laminated isotropic construction.

For plate-buckling applications, the material comparison is shown in figure 16(a). This figure indicates that the E-glass filament and epoxy resin plate would weigh about 2 percent more than an aluminum plate.

If compressive crushing is the basis for comparison, the material efficiency parameter is ρ/σ_y. Values of ρ/σ_y for the materials considered herein are shown in figure 16(b). Examination of figure 16(b) indicates that a nonbuckling structural element of E-glass filaments and epoxy resin subjected to a compressive load would weigh approximately 4 percent more than an aluminum structure and only 55 percent of the weight of a magnesium structure.

When the maximum strength of a buckled plate is the basis for comparison, an approximate material efficiency parameter is $\frac{\rho}{(E\sigma_y)^{1/4}}$. Values of $\frac{\rho}{(E\sigma_y)^{1/4}}$ for the

TABLE IV.- MATERIAL PROPERTIES

Material	ρ		E		σ_y	
	lbm/in^3	Mg/m^3	ksi	GN/m^2	ksi	MN/m^2
E-glass and epoxy[a]	0.067	1.85	2 870	19.8	[b]24 to [c]45	166 to 310
Aluminum	.101	2.79	10 400	71.7	72	496
Magnesium	.065	1.80	6 400	44.1	23	159
Titanium	.160	4.42	17 000	117.0	130	896
Beryllium (cross rolled)	.067	1.85	44 000	303.0	60	414

[a]Experimentally determined properties.

[b]The edge stress at failure for a buckled plate with a b/t ratio of 30.

[c]The compressive strength of the dog bone type of specimen.

materials considered in the comparison are shown in figure 16(c). Two values of the parameter are shown in figure 16(c) for the E-glass filament and epoxy resin composite material. The lower value is based on a compressive strength of 45 ksi (310 MN/m^2) which is the stress at which delamination occurred in the absence of buckling for the dog bone type of specimens. The upper value is based on a compressive strength of 24 ksi (166 MN/m^2) which is the edge stress at failure for a buckled plate with a b/t ratio of 30. The two values shown are for two extremes in plate design.

A comparison over a wide range of plate designs is shown by the efficiency plot in figure 17 where the weight parameter $\rho t/b$ is plotted as a function of the structural index N_x/b. On this figure the test data for the E-glass and epoxy plates are compared with data for aluminum plates obtained from reference 15. The solid line on the figure represents the yield stress of 72 ksi (496 MN/m^2) for the aluminum alloy while the dashed line is based upon a stress of 45 ksi (310 MN/m^2) determined from the compression test of dog bone type of specimens. For high values of the structural index the aluminum plate weighs somewhat less than the E-glass and epoxy plate as was shown by the previous material efficiency parameter comparison. However, at intermediate values of the structural index, the weights of the two types of plates are comparable. At lower values of the structural index shown in the figure, the weight advantage again favors the aluminum plate. Since the failure of the E-glass and epoxy plates was presumably governed by the shear strength, an improvement in the shear capability might favor this material such that its efficiency could exceed that of the aluminum alloy.

CONCLUDING REMARKS

The compressive behavior of glass-filament-reinforced plates of laminated isotropic construction has been investigated. Young's modulus in compression for the plates tested was in reasonable agreement with theoretical predictions. The experimentally determined and theoretical buckling stresses of the plates were in excellent agreement. The stress—unit-shortening curve for a plate in the post-buckling region can adequately be predicted by conventional theory for metallic plates. Failure of the plates was observed to be a consequence of delamination and occurred for loadings lower than the theoretical maximum strength predicted by an effective width formula that is often used to predict the maximum strength of metallic plates. In using an effective width formula to predict maximum strength, it was assumed that failure occurs when the edge stress of the buckled plate equals the delamination stress of the unbuckled compression test specimen. The E-glass filament and epoxy resin composite material used in the study reported herein is comparable, as a lightweight material, with aluminum in plate-buckling and crushing-strength applications.

Langley Research Center,
National Aeronautics and Space Administration,
Langley Station, Hampton, Va., November 9, 1966,
124-08-01-10-23.

APPENDIX

CONVERSION OF U.S. CUSTOMARY UNITS TO SI UNITS

The International System of Units (SI) was adopted by the Eleventh General Conference on Weights and Measures, Paris, October 1960, in Resolution No. 12 (ref. 5). Conversion factors for the units used herein are given in the following table:

Physical quantity	U.S. Customary Unit	Conversion factor (*)	SI Unit
Length	in.	0.0254	meters (m)
Temperature	(^{o}F + 460)	5/9	degrees Kelvin (^{o}K)
Density	lbm/in^3	27.68×10^3	kilograms per cubic meter (kg/m^3)
Modulus, stress	psi = lbf/in^2	6895	newtons per square meter (N/m^2)

*Multiply value given in U.S. Customary Units by conversion factor to obtain equivalent value in SI Unit.

Prefixes to indicate multiple of units are as follows:

Prefix	Multiple
micro (μ)	10^{-6}
centi (c)	10^{-2}
kilo (k)	10^3
mega (M)	10^6
giga (G)	10^9

REFERENCES

1. Fried, N.; and Winans, R. R.: Compressive Strength of Parallel Filament-Reinforced Plastics: Development of a New Test Method. Symposium on Standards for Filament-Wound Reinforced Plastics, Spec. Tech. Publ. No. 327, Am. Soc. Testing Mater., 1962, pp. 83-95.

2. Fried, N.: The Response of Orthogonal Filament Wound Materials to Compressive Stress. Proceedings 20th Anniversary Technical Conference, Reinforced Plastics Div., Soc. Plastics Ind., Inc., Feb. 1965.

3. Dow, Norris F.; and Rosen, B. Walter: Evaluations of Filament-Reinforced Composites for Aerospace Structural Applications. NASA CR-207, 1965.

4. Card, Michael F.: Experiments To Determine Elastic Moduli for Filament-Wound Cylinders. NASA TN D-3110, 1965.

5. Mechtly, E. A.: The International System of Units – Physical Constants and Conversion Factors. NASA SP-7012, 1964.

6. Werren, Fred; and Norris, C. B.: Mechanical Properties of a Laminate Designed To Be Isotropic. Rept. No. 1841, Forest Prod. Lab., U. S. Dept. Agriculture, May 1953.

7. Anon.: 1965 Book of ASTM Standards With Related Material. Part 27 – Plastics – General Methods of Testing. Am. Soc. Testing Mater., c.1965.

8. Hu, Pai C.; Lundquist, Eugene E.; and Batdorf, S. B.: Effect of Small Deviations From Flatness on Effective Width and Buckling of Plates in Compression. NACA TN 1124, 1946.

9. Greszczuk, Longin B.: Theoretical and Experimental Studies on Properties and Behavior of Filamentary Composites. Proceedings 21st Annual Technical and Management Conference, Reinforced Plastics Div., Soc. Plastics Ind., Inc., Feb. 1966.

10. Rosen, B. Walter; Dow, Norris F.; and Hashin, Zvi: Mechanical Properties of Fibrous Composites. NASA CR-31, 1964.

11. Dietz, Albert G. H., ed.: Engineering Laminates. John Wiley & Sons, Inc., 1949.

12. Libove, Charles; and Stein, Manuel: Charts for Critical Combinations of Longitudinal and Transverse Direct Stress for Flat Rectangular Plates. NACA WR L-224, 1946. (Formerly NACA ARR L6A05.)

13. Stowell, Elbridge Z.: A Unified Theory of Plastic Buckling of Columns and Plates. NACA Rept. 898, 1948. (Supersedes NACA TN 1556.)

14. Peterson, James P.; Whitley, Ralph O.; and Deaton, Jerry W.: Structural Behavior and Compressive Strength of Circular Cylinders With Longitudinal Stiffening. NASA TN D-1251, 1962.

15. Anderson, Roger A.; and Anderson, Melvin S.: Correlation of Crippling Strength of Plate Structures With Material Properties. NACA TN 3600, 1956.

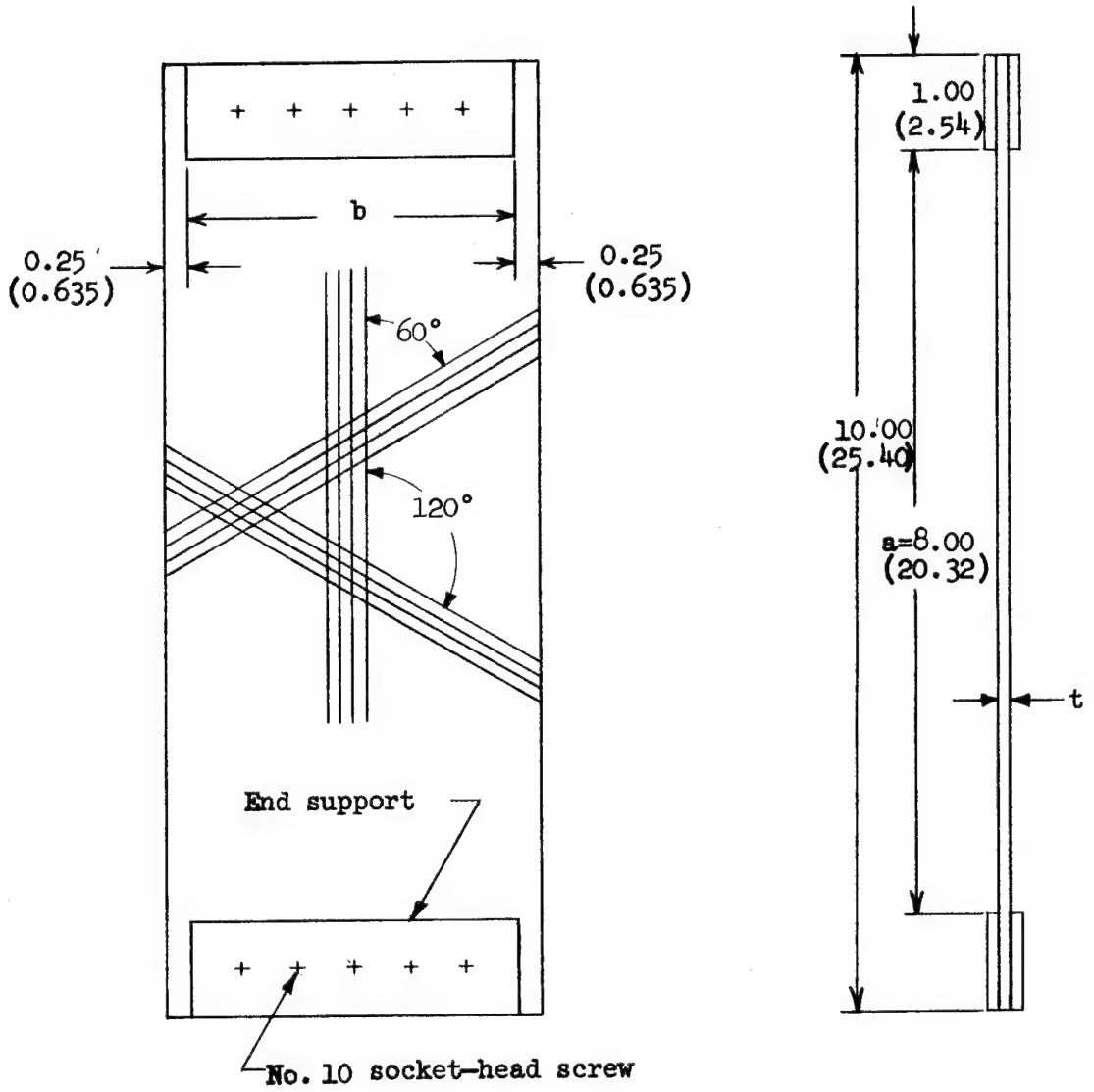

(a) Front view.

(b) Side view.

Figure 1.- Details of test specimen. All dimensions are given in inches (cm).

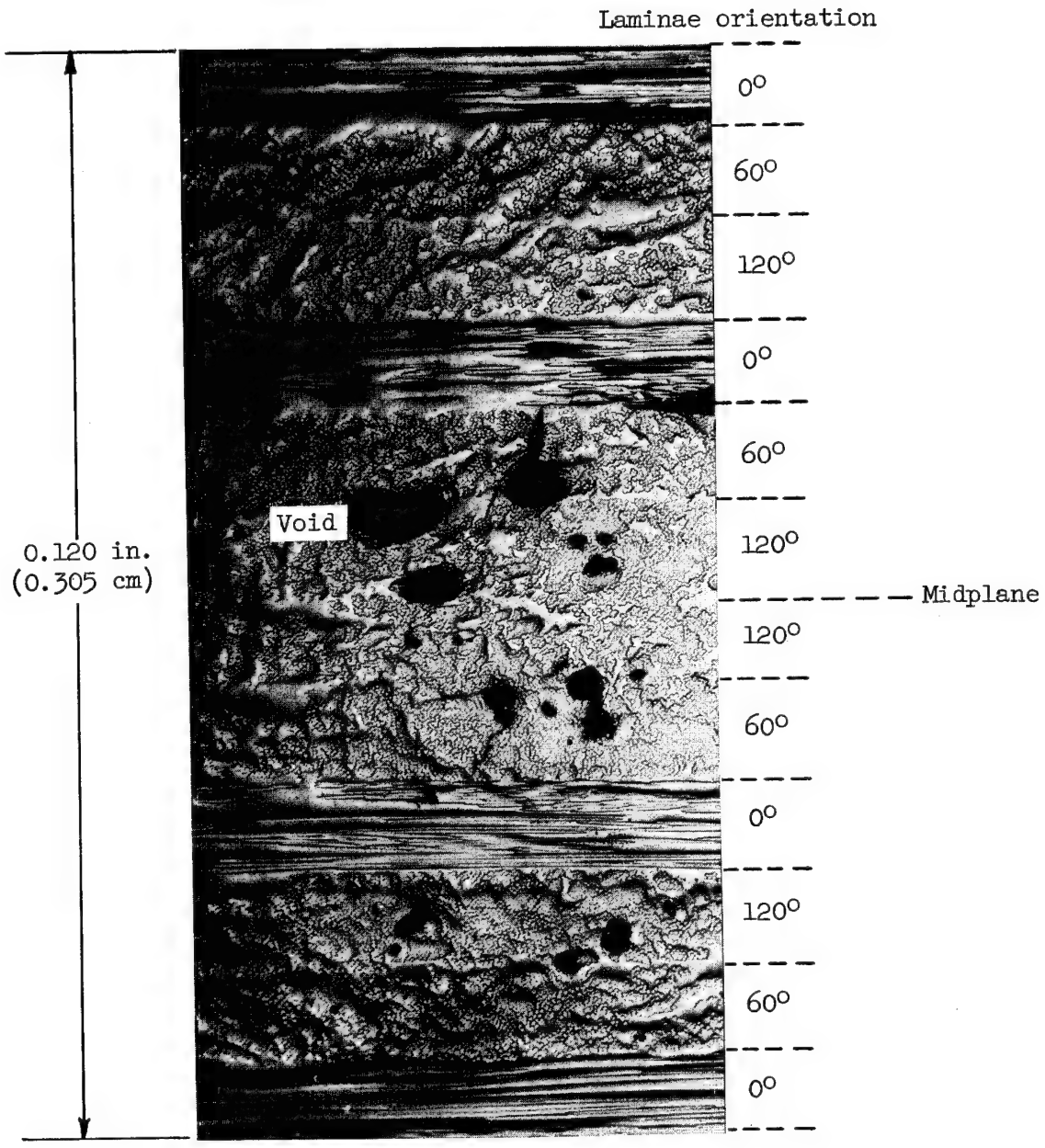

Figure 2.- Photomicrograph of plate cross section.

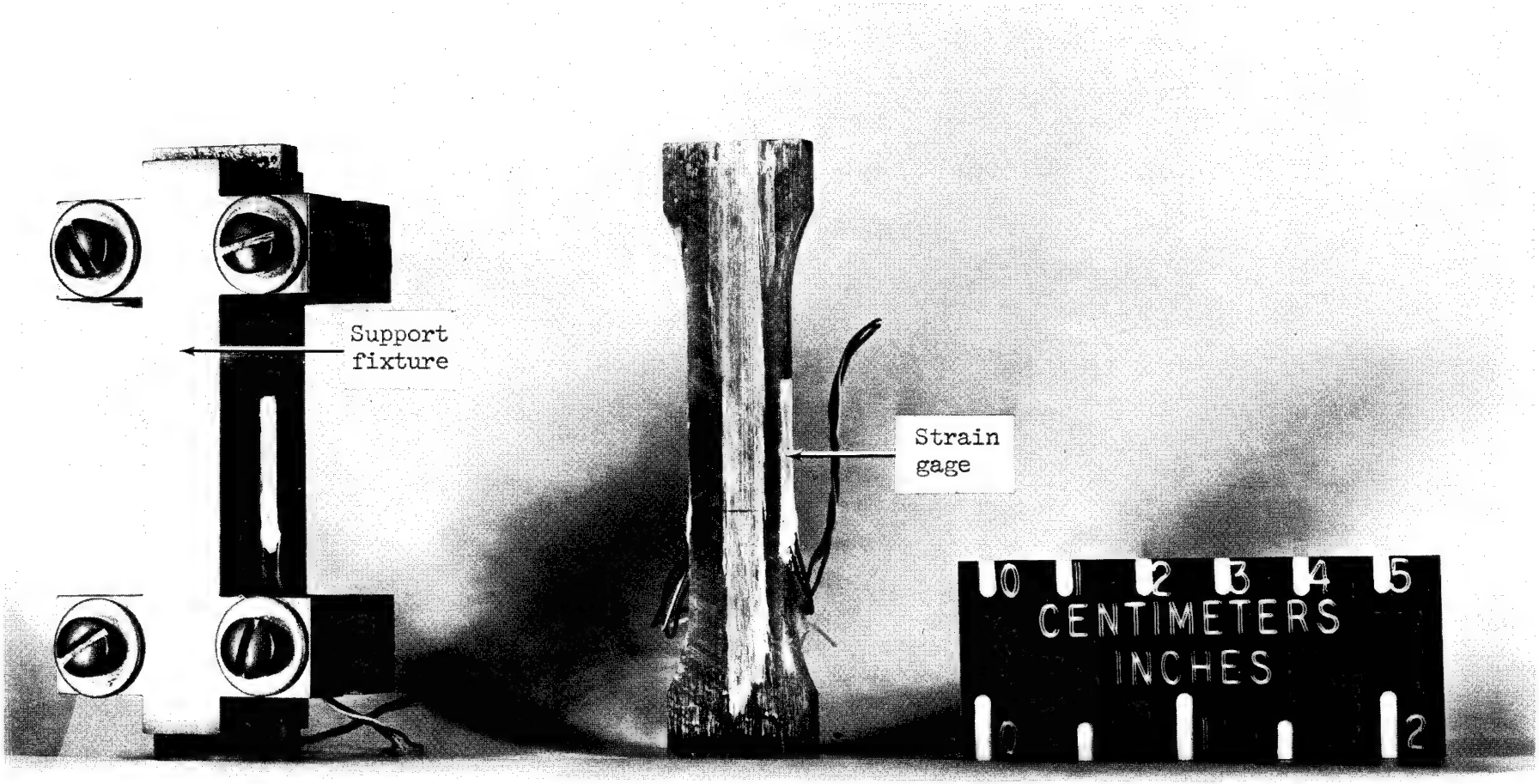

Figure 3.- Dog bone type of compression specimen and support fixture. L-66-5902.1

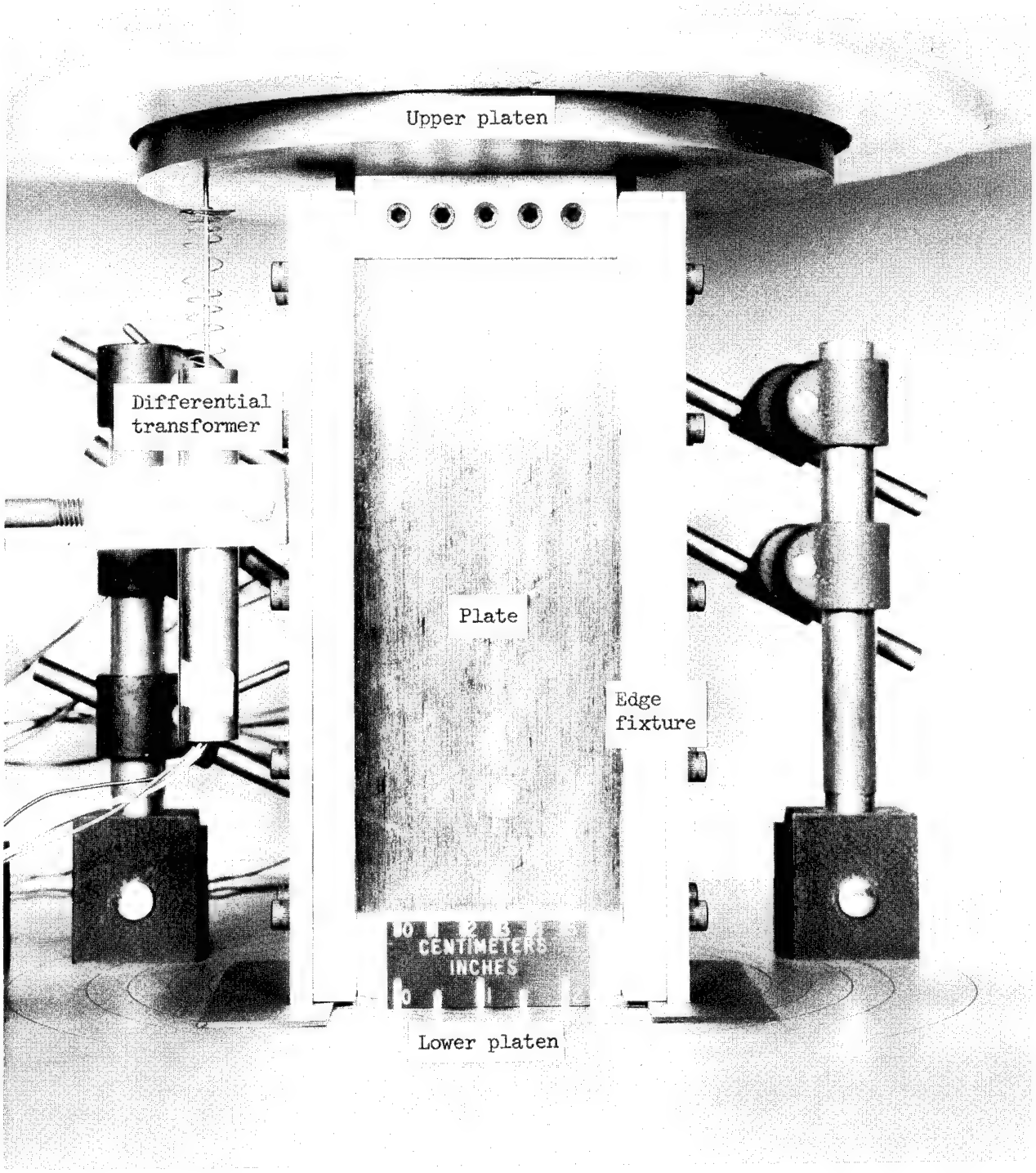

Figure 4.- Plate installed in test machine.

L-66-4886.1

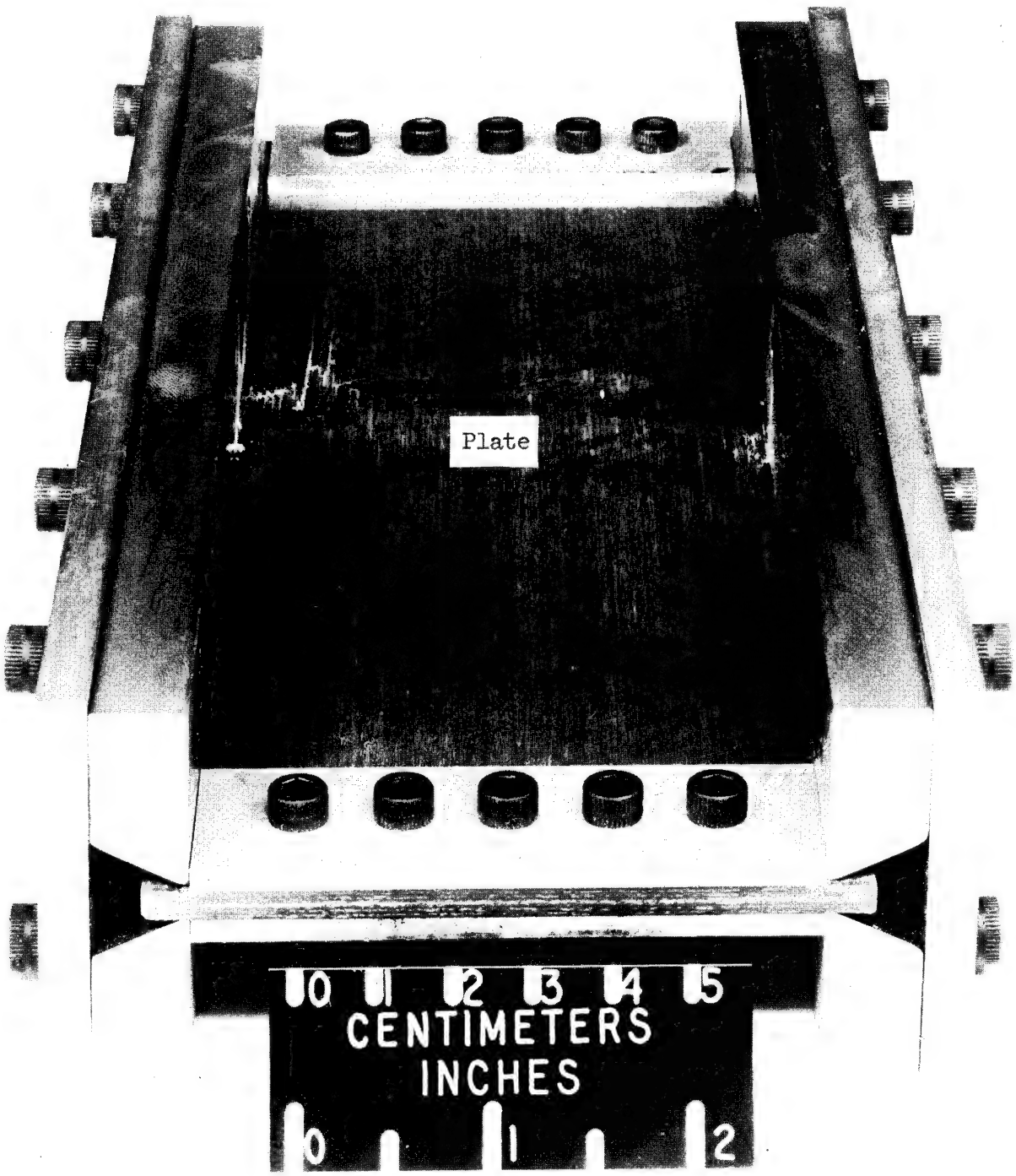

Figure 5.- Edge fixtures.

L-66-4884.1

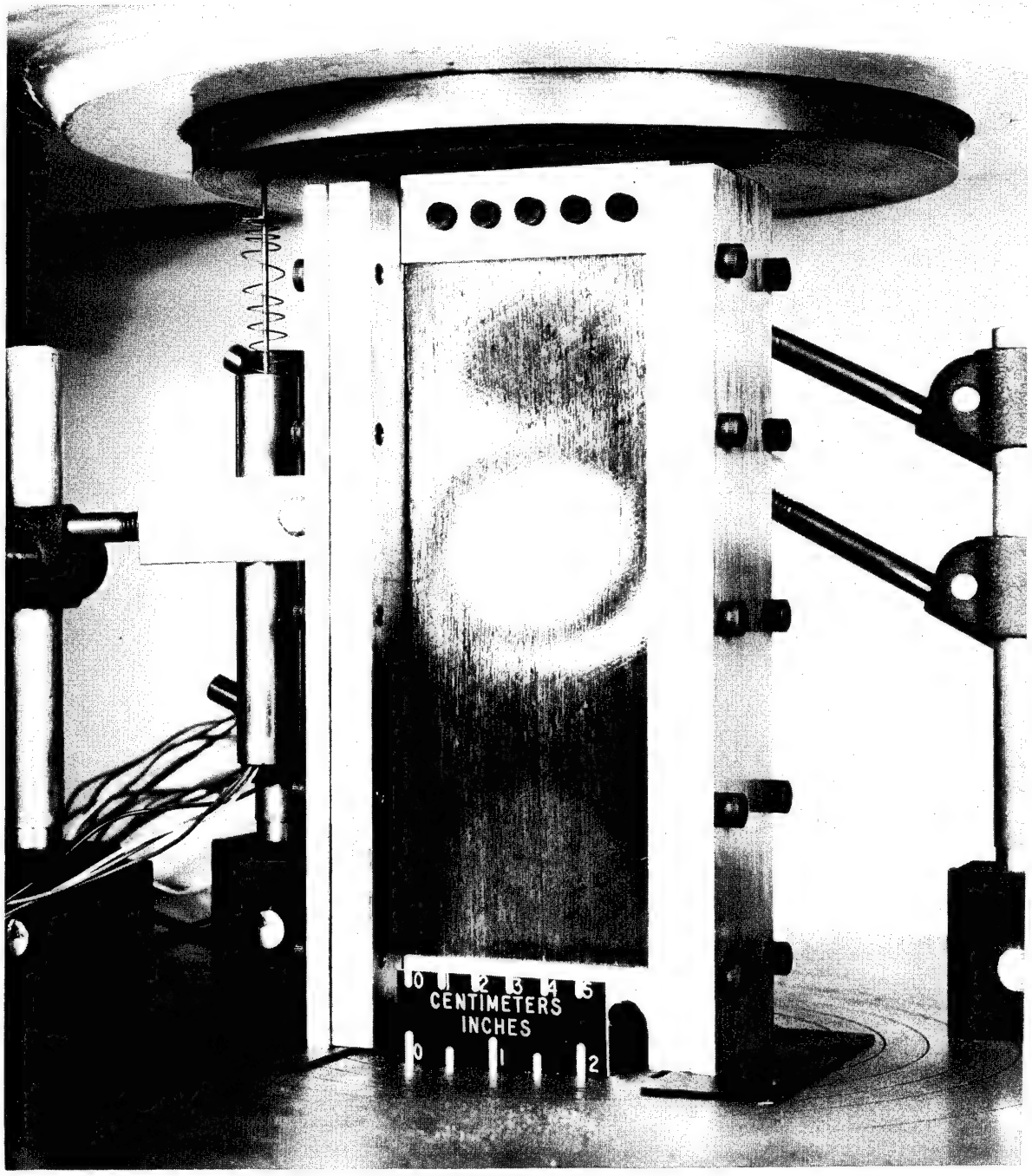

Figure 6.- Buckled plate.

L-66-4888

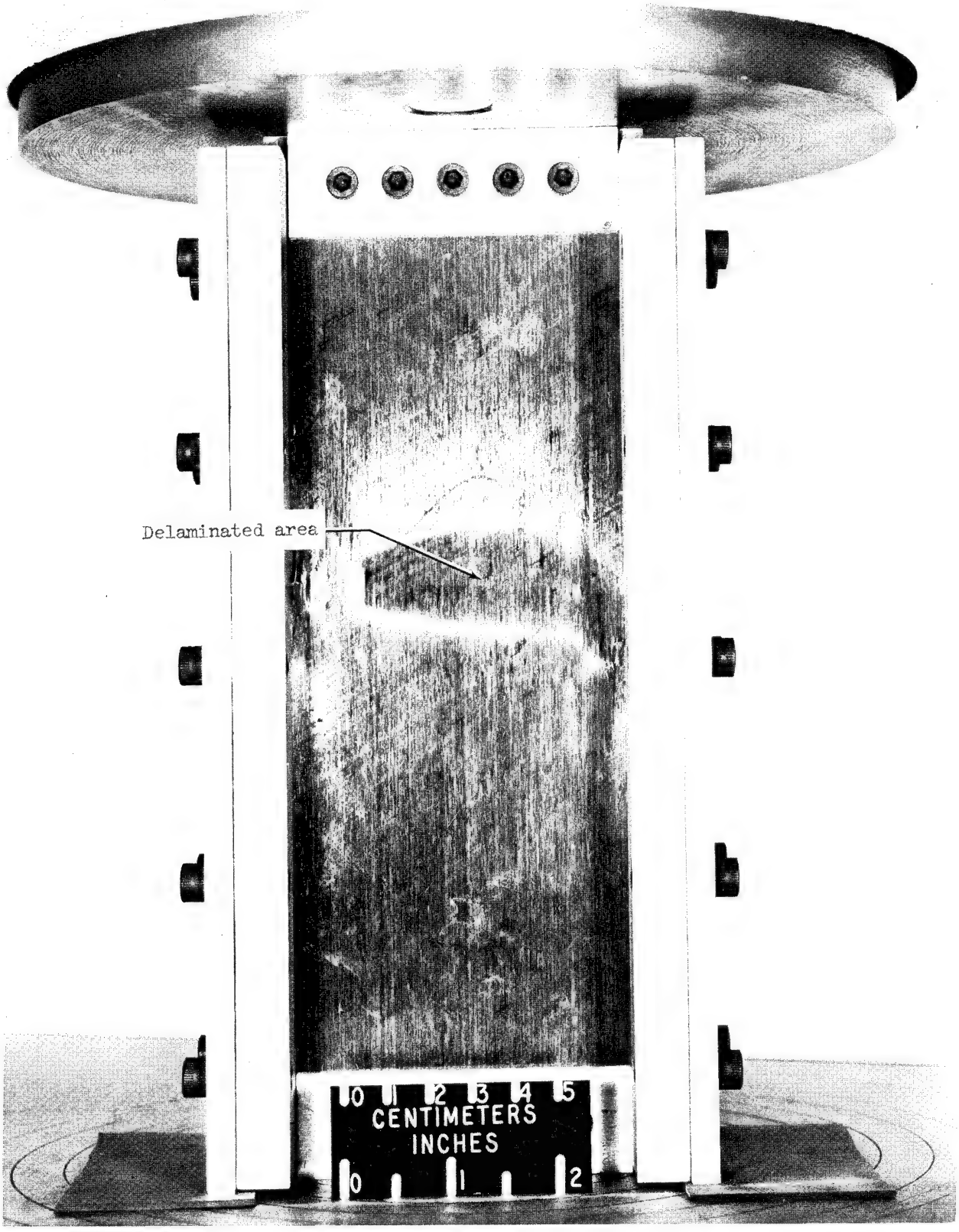

Figure 7.- Failed plate.

L-66-5701.1

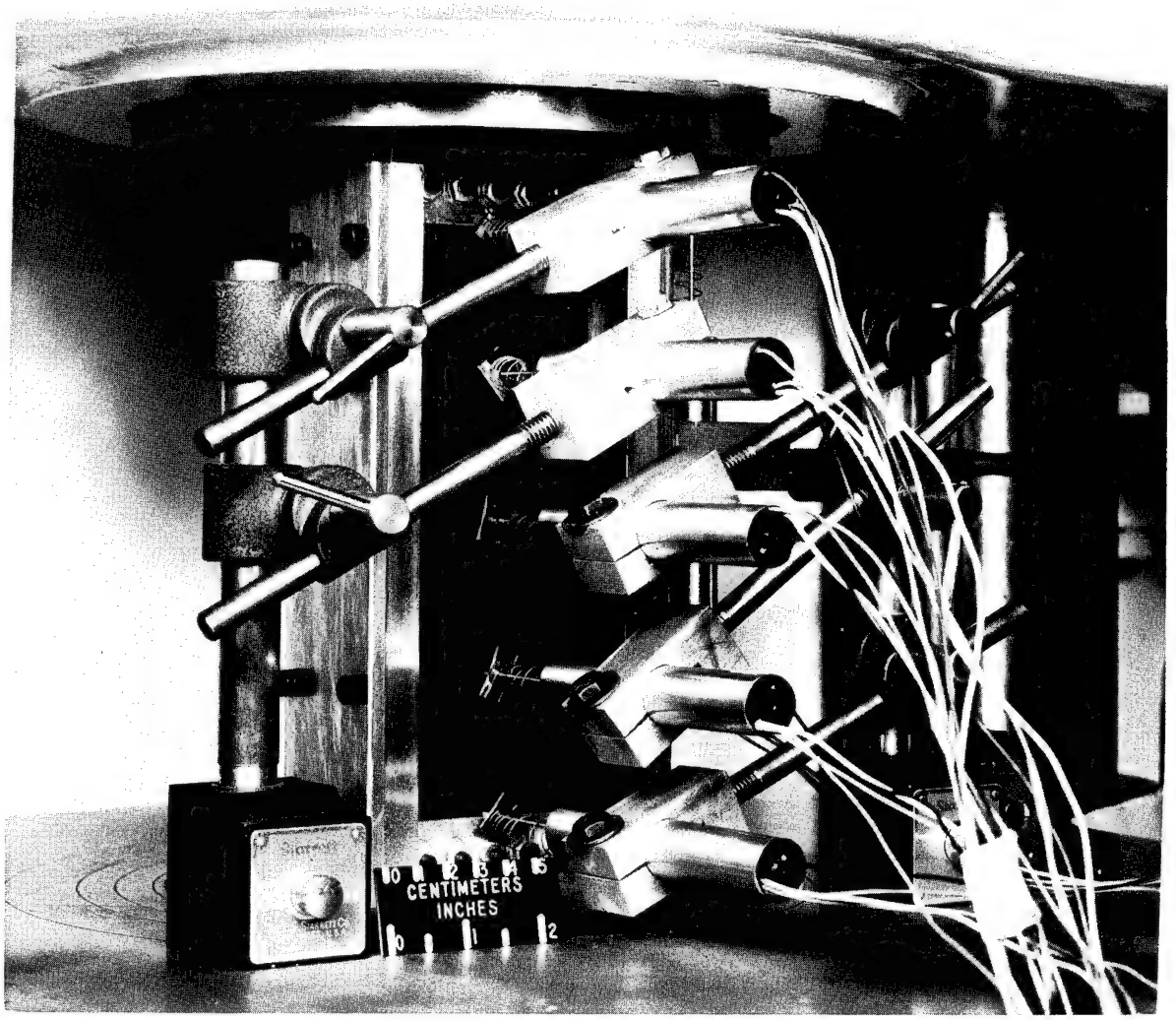

Figure 8.- Instrumentation used to measure lateral deflection of plates. L-66-4889

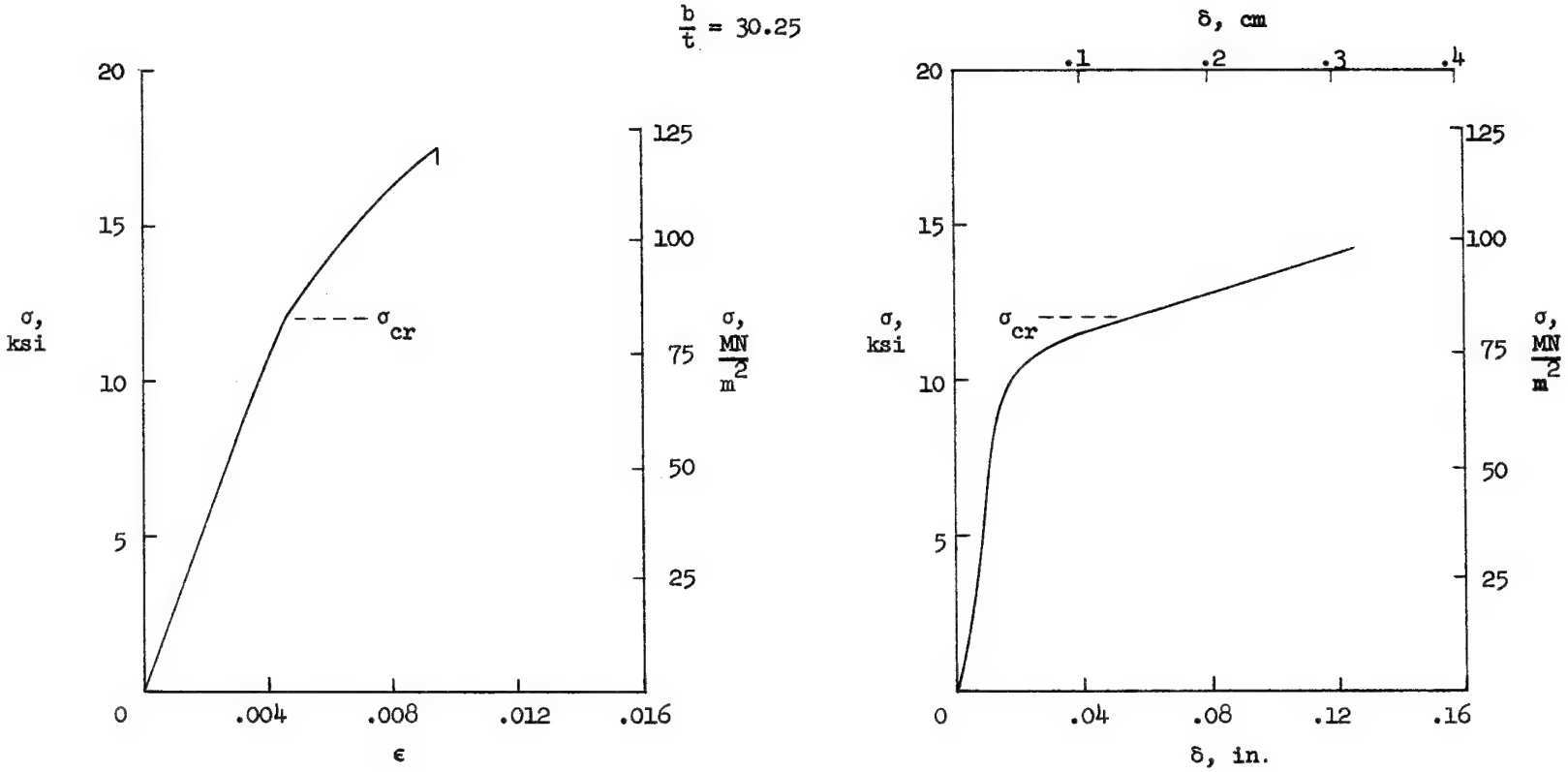

Figure 9.- Variation of stress with unit-shortening and buckle amplitude for plate 1.

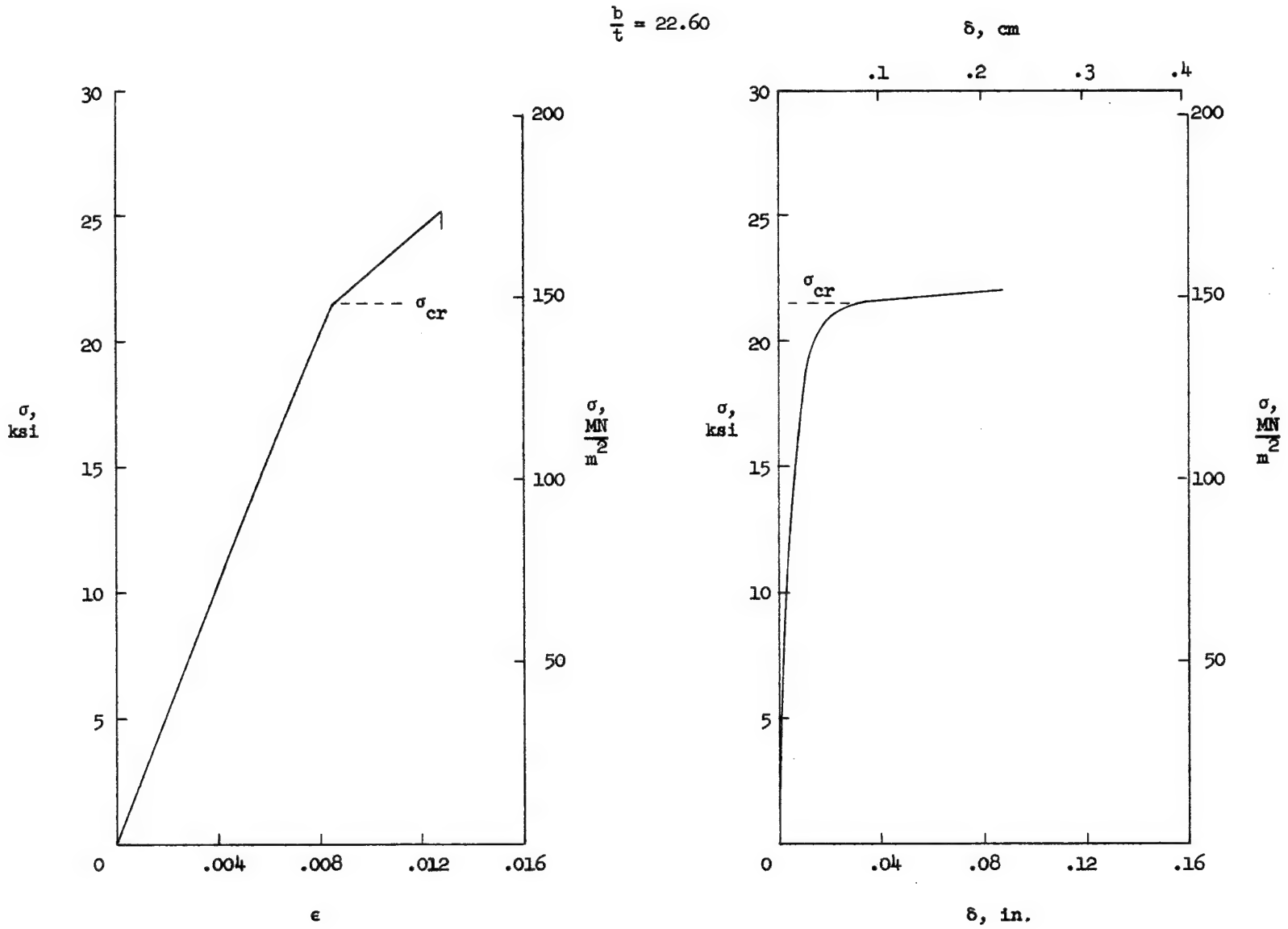

Figure 10.- Variation of stress with unit-shortening and buckle amplitude for plate 9.

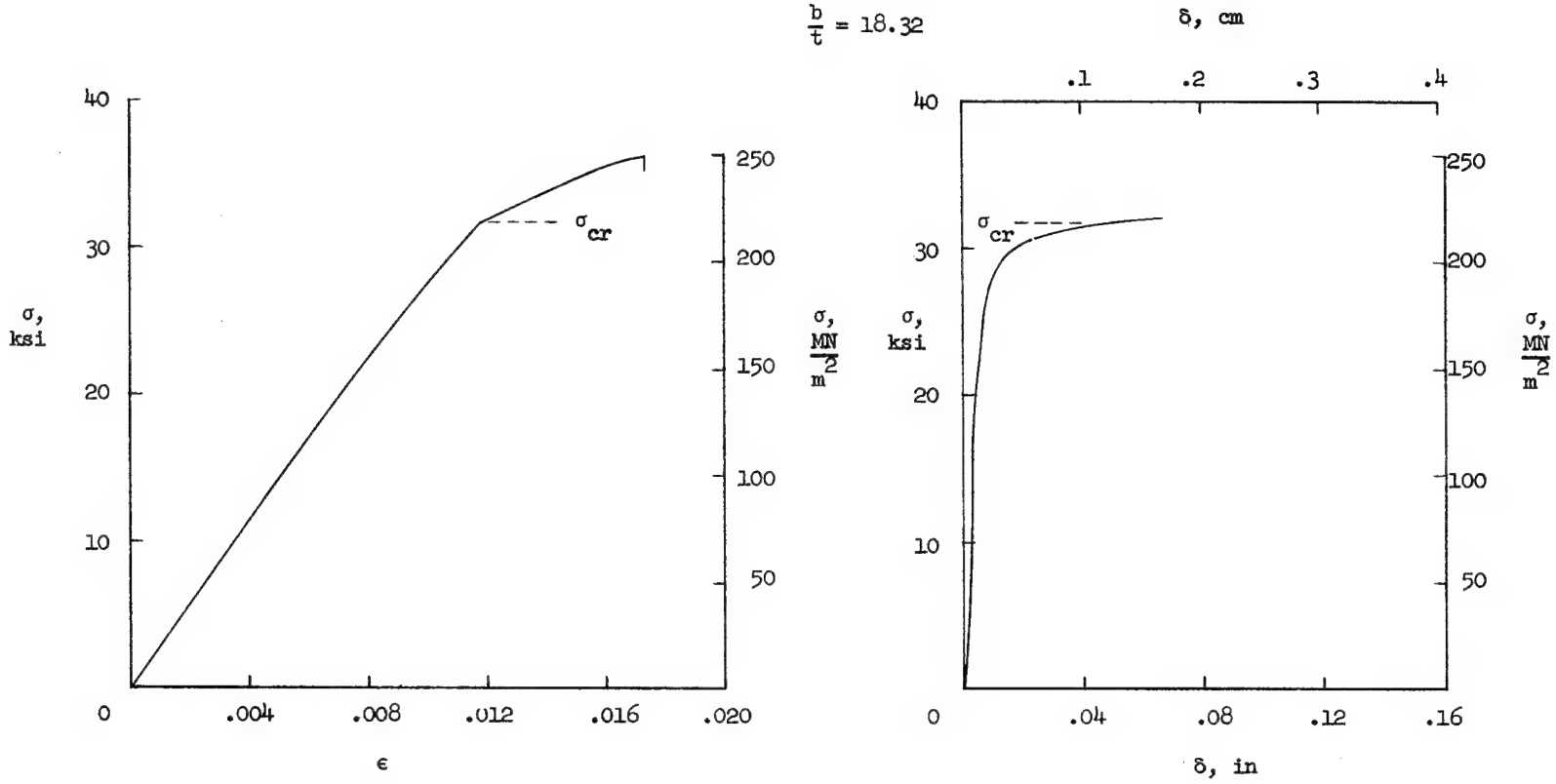

Figure 11.- Variation of stress with unit-shortening and buckle amplitude for plate 14.

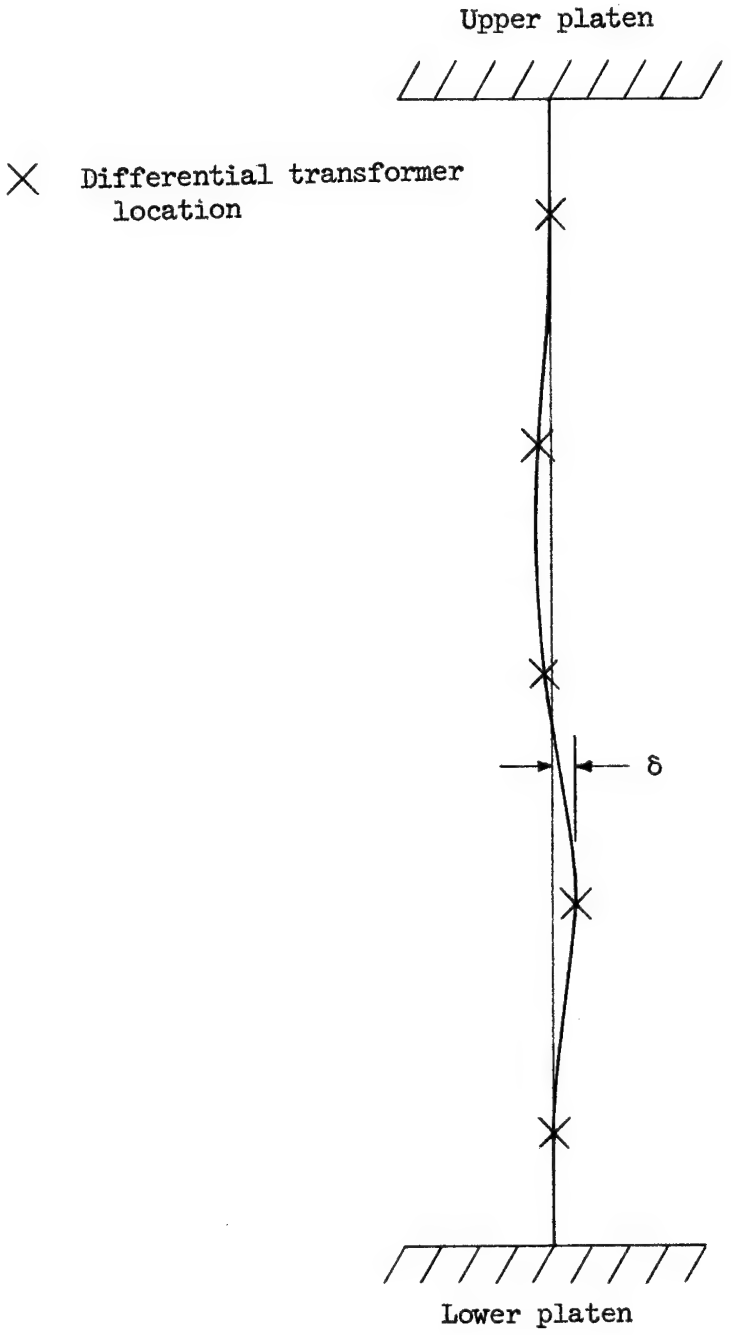

Figure 12.- Schematic of buckle pattern.

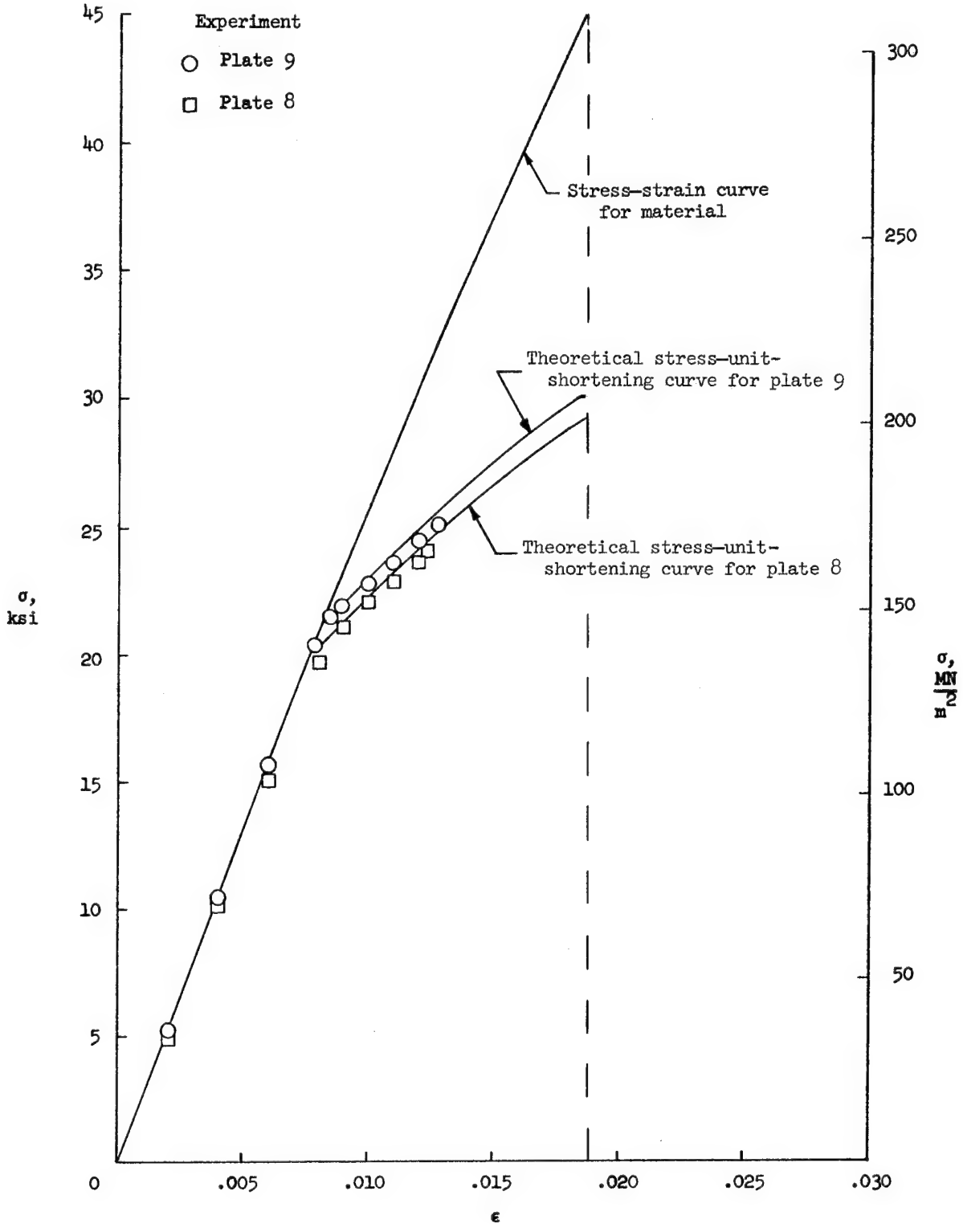

Figure 13.- Comparison of experimental and theoretical stress—unit-shortening curves.

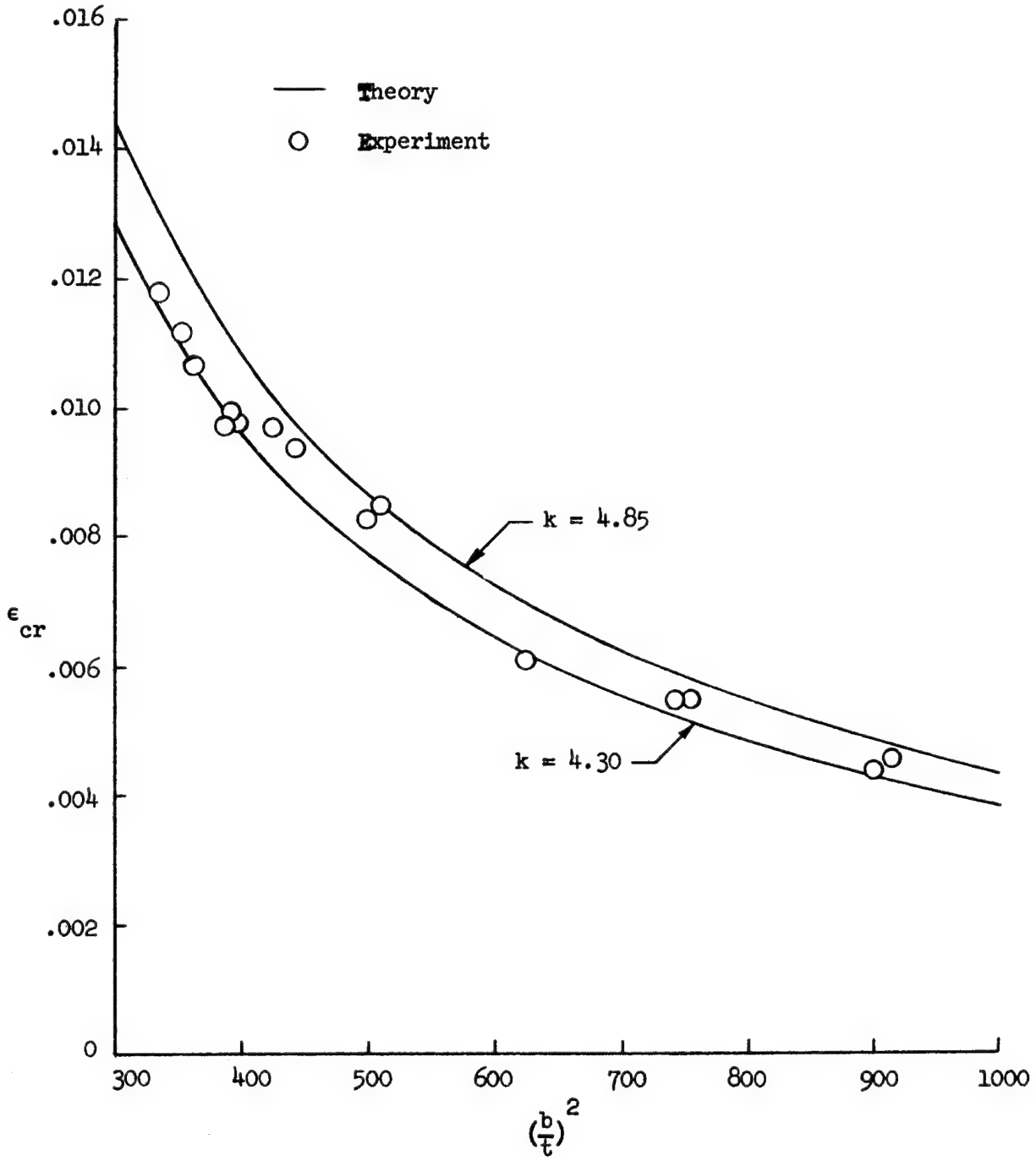

Figure 14.- Comparison of buckling data and theory.

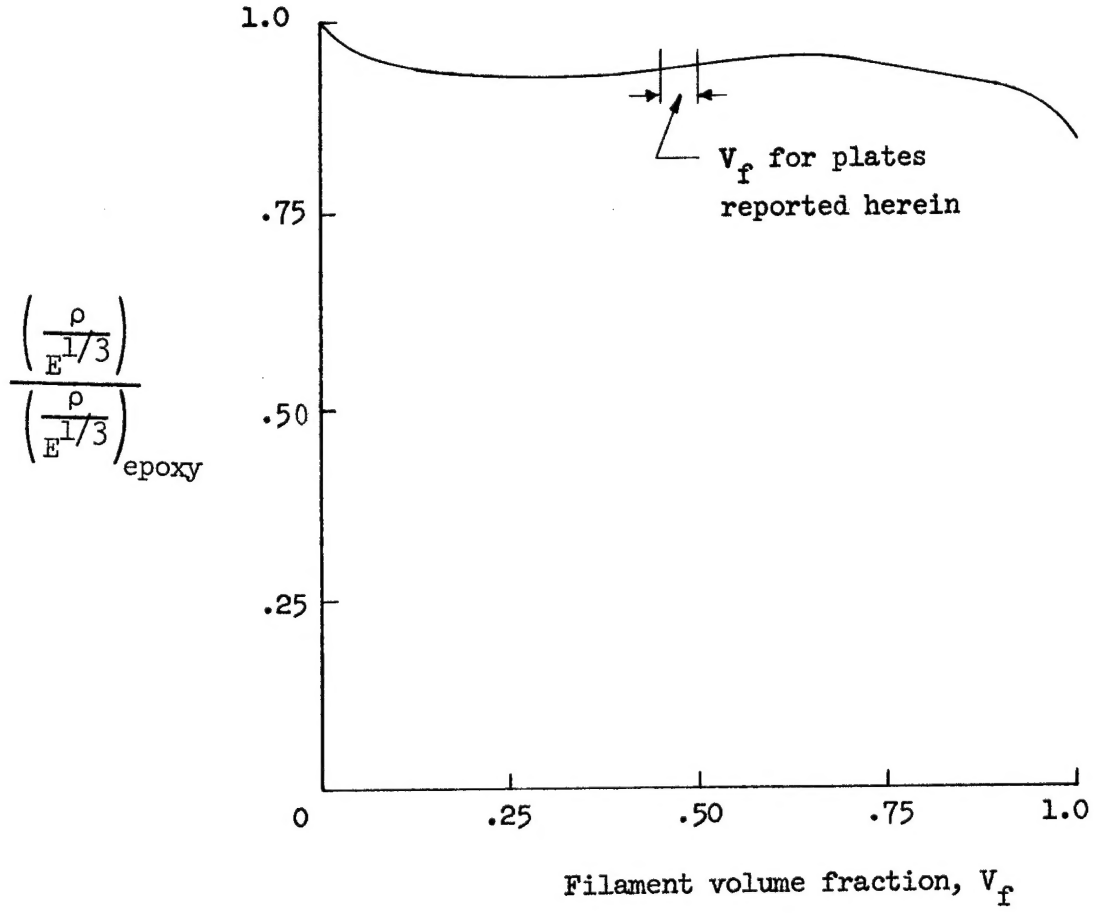

Figure 15.- Effect of filament volume fraction on material efficiency for an E-glass epoxy isotropic plate.

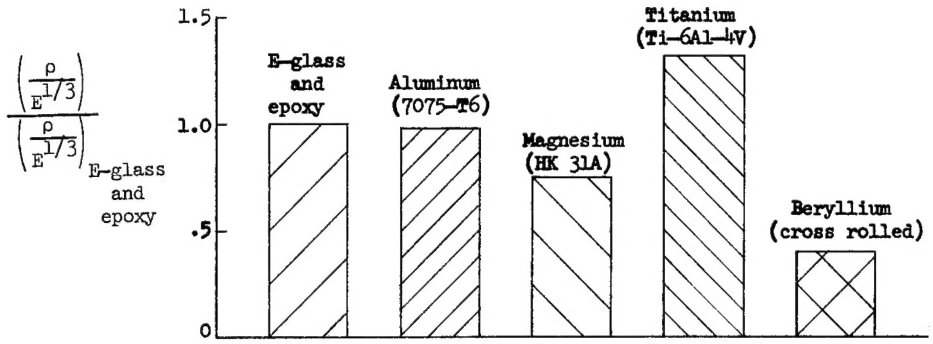

(a) Plate buckling.

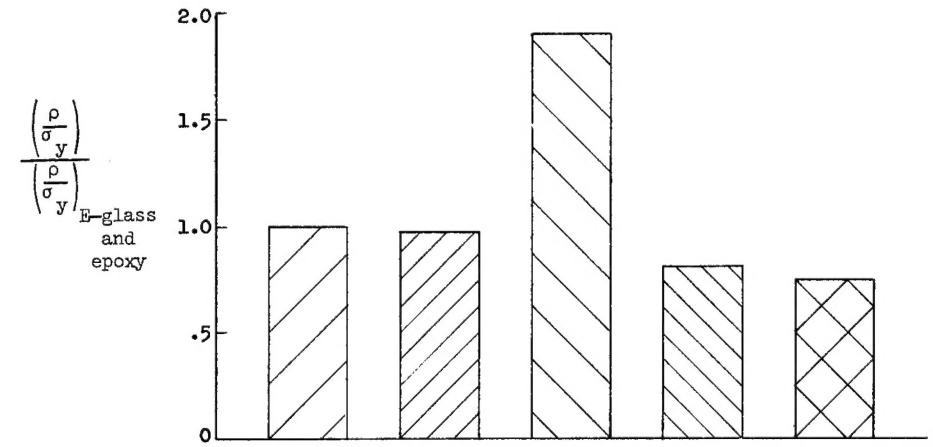

(b) Compressive strength.

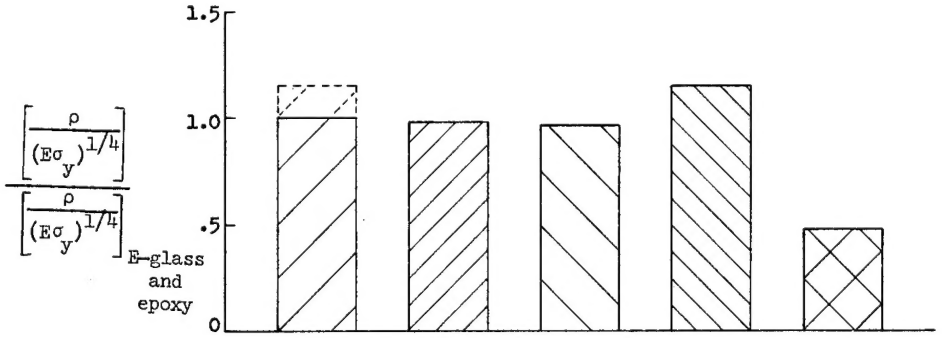

(c) Maximum strength of a buckled plate.

Figure 16.- Materials comparison.

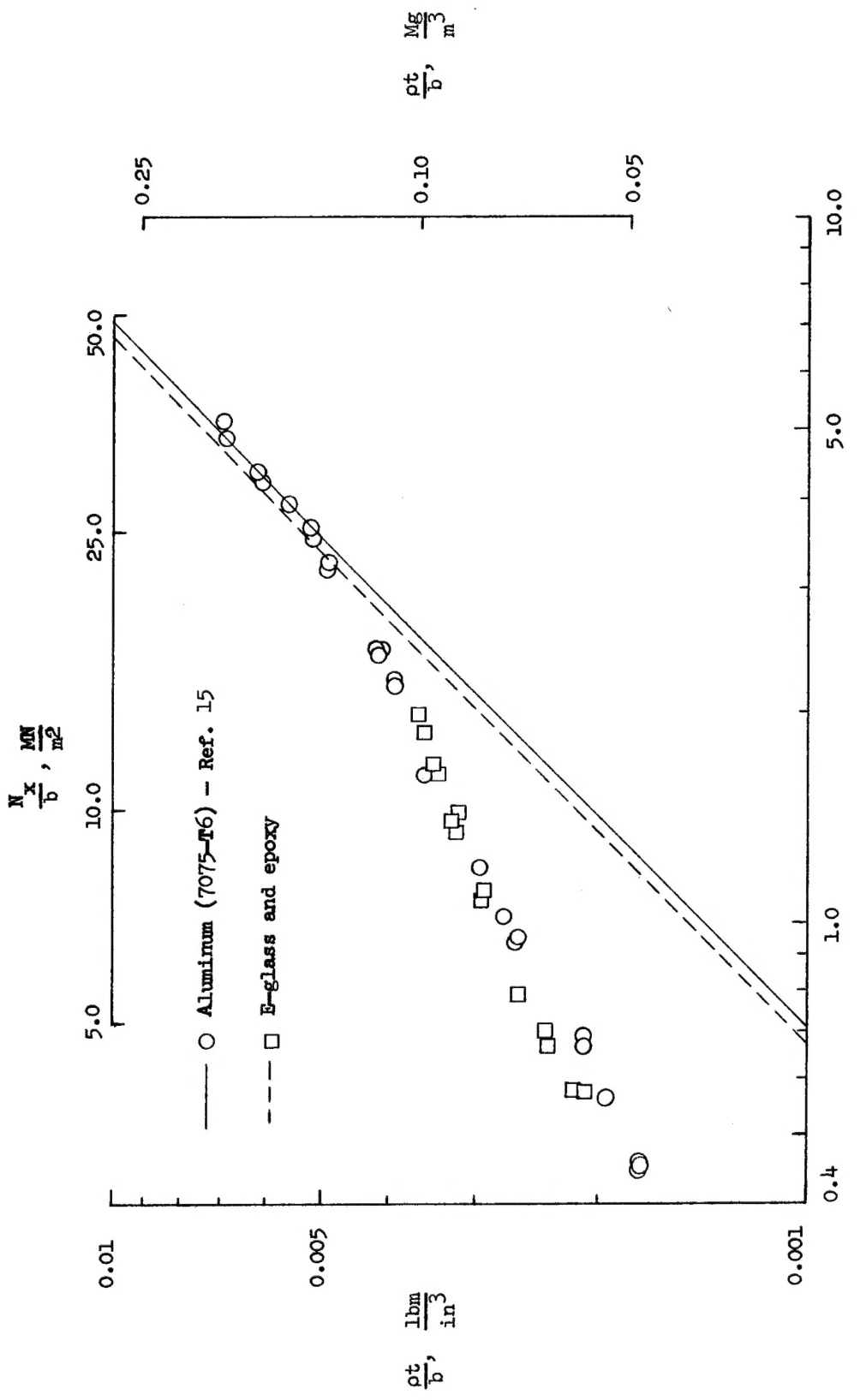

Figure 17.- Weight-efficiency comparison of an E-glass and epoxy composite material with aluminum.

NASA-Langley, 1967 —— 18

"The aeronautical and space activities of the United States shall be conducted so as to contribute . . . to the expansion of human knowledge of phenomena in the atmosphere and space. The Administration shall provide for the widest practicable and appropriate dissemination of information concerning its activities and the results thereof."

—NATIONAL AERONAUTICS AND SPACE ACT OF 1958

NASA SCIENTIFIC AND TECHNICAL PUBLICATIONS

TECHNICAL REPORTS: Scientific and technical information considered important, complete, and a lasting contribution to existing knowledge.

TECHNICAL NOTES: Information less broad in scope but nevertheless of importance as a contribution to existing knowledge.

TECHNICAL MEMORANDUMS: Information receiving limited distribution because of preliminary data, security classification, or other reasons.

CONTRACTOR REPORTS: Scientific and technical information generated under a NASA contract or grant and considered an important contribution to existing knowledge.

TECHNICAL TRANSLATIONS: Information published in a foreign language considered to merit NASA distribution in English.

SPECIAL PUBLICATIONS: Information derived from or of value to NASA activities. Publications include conference proceedings, monographs, data compilations, handbooks, sourcebooks, and special bibliographies.

TECHNOLOGY UTILIZATION PUBLICATIONS: Information on technology used by NASA that may be of particular interest in commercial and other non-aerospace applications. Publications include Tech Briefs, Technology Utilization Reports and Notes, and Technology Surveys.

Details on the availability of these publications may be obtained from:

SCIENTIFIC AND TECHNICAL INFORMATION DIVISION

NATIONAL AERONAUTICS AND SPACE ADMINISTRATION

Washington, D.C. 20546